Numerical approaches for investigating the chaotic behavior of nonlinear disordered lattice models

Haris Skokos

**Department of Mathematics and Applied Mathematics
University of Cape Town, South Africa**

**E-mail: haris.skokos@uct.ac.za
URL: http://math_research.uct.ac.za/~hskokos/**

Isaac Newton Institute
for Mathematical Sciences

Outline

- **The one-dimensional quartic disordered Klein-Gordon (1D DKG) model: Different dynamical regimes**

- **Maximum Lyapunov Exponent (MLE): strength of chaos**

- **Deviation Vector Distributions (DVDs): mechanisms of chaotic spreading**

- **Frequency Map Analysis (FMA): characteristics of spatiotemporal evolution of chaos**

- **Generalized Alignment Index (GALI): localized vs. spreading chaos**

- **Summary**

The one-dimensional disordered Klein Gordon model (1D DKG)

$$H = \sum_{l=1}^{N} \frac{p_l^2}{2} + \frac{\tilde{\varepsilon}_l}{2} u_l^2 + \frac{1}{4} u_l^4 + \frac{1}{2W} (u_{l+1} - u_l)^2$$

with **fixed boundary conditions** $u_0 = p_0 = u_{N+1} = p_{N+1} = 0$. **Typically N=1000.**

Parameters: W and the **total energy H.** $\tilde{\varepsilon}_l$ chosen uniformly from $\left[\frac{1}{2}, \frac{3}{2}\right]$.

Linear case (neglecting the term $u_l^4/4$)

Ansatz: $u_l = A_l \exp(i\omega t)$. **Normal modes (NMs) $A_{v,l}$ - Eigenvalue problem:**

$$\lambda A_l = \varepsilon_l A_l - (A_{l+1} + A_{l-1}) \text{ with } \lambda = W\omega^2 - W - 2, \quad \varepsilon_l = W(\tilde{\varepsilon}_l - 1)$$

Anderson localization [Anderson, Phys. Rev. (1958)]. **Experiments on BEC** [Billy et al., Nature (2008)]

What happens in the presence of nonlinearity?

Will nonlinearity destroy localization?

Characteristics of energy distributions

We consider normalized **energy distributions** $\xi_l = \dfrac{H_l}{\sum_m H_m}$

with $H_l = \dfrac{p_l^2}{2} + \dfrac{\tilde{\varepsilon}_l}{2} u_l^2 + \dfrac{1}{4} u_l^4 + \dfrac{1}{4W}(u_{l+1} - u_l)^2$

Second moment: $m_2 = \displaystyle\sum_{l=1}^{N} (l - \bar{l})^2 \, \xi_l$ with $\bar{l} = \displaystyle\sum_{l=1}^{N} l \xi_l$

Participation number: $P = \dfrac{1}{\sum_{l=1}^{N} \xi_l^2}$

measures the number of stronger excited sites in ξ_l.

Single site $P=1$. Equipartition of energy $P=N$.

Different dynamical regimes

Three expected evolution regimes [Flach, Chem. Phys (2010) - S. & Flach, PRE (2010) - Laptyeva et al., EPL (2010) - Bodyfelt et al., PRE (2011)]

Δ: **width of the frequency spectrum.** $\Delta = 1 + \frac{4}{W}$ **since** $\omega_\nu^2 \in \left[\frac{1}{2}, \frac{3}{2} + \frac{4}{W}\right]$

d: average spacing of interacting modes. $d \approx \frac{\Delta}{V}$,

V: **localization volume of an eigenstate** $V \sim \frac{1}{\sum_{l=1}^{N} A_{\nu,l}^4}$

δ: **nonlinear frequency shift.** $\delta_l = \frac{3H_l}{2\tilde{\varepsilon}_l} \propto H$

Weak Chaos Regime: $\delta < d, \ m_2 \propto t^{1/3} \ (P \propto t^{1/6})$

Frequency shift is less than the average spacing of interacting modes. NMs are weakly interacting with each other. [Molina, PRB (1998) – Pikovsky & Shepelyansky, PRL (2008) – Flach et al., PRL (2009)].

Strong Chaos Regime: $d < \delta < \Delta, \ m_2 \propto t^{1/2} \ (P \propto t^{1/4}) \rightarrow m_2 \propto t^{1/3}$

Almost all NMs in the packet are resonantly interacting. Wave packets initially spread faster and eventually enter the weak chaos regime.

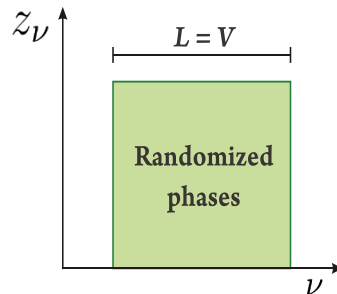**Selftrapping Regime:** $\delta > \Delta$

Frequency shift exceeds the spectrum width. Frequencies of excited NMs are tuned out of resonances with the nonexcited ones, leading to selftrapping, while a small part of the wave packet subdiffuses [Kopidakis et al., PRL (2008)].
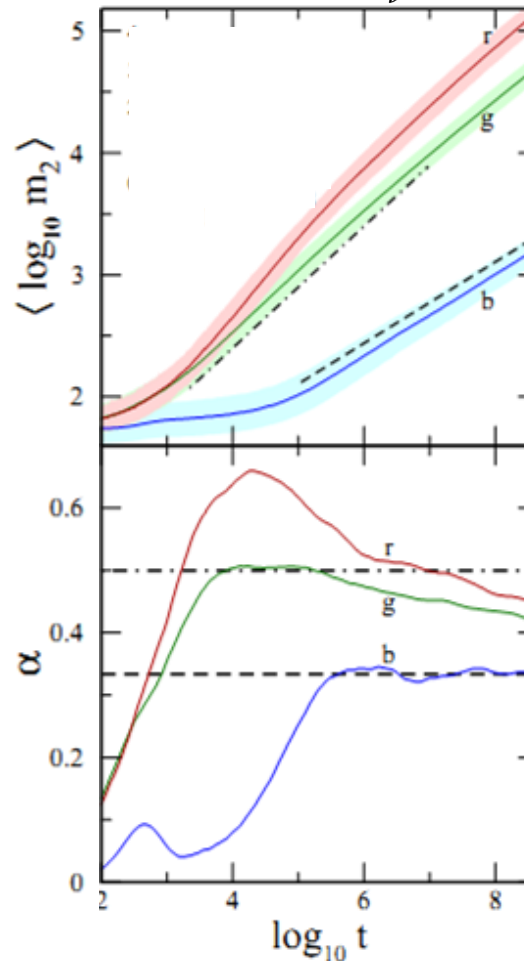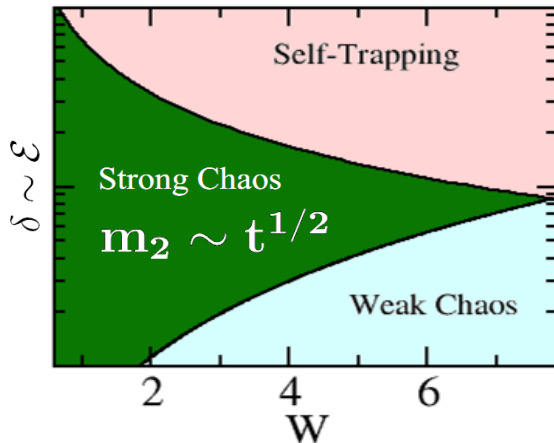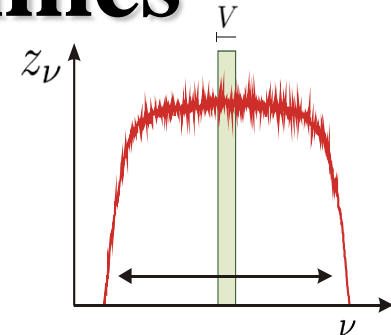
Strong and weak chaos regimes

We consider **compact initial wave packets of width *L*** [Laptyeva et al., EPL (2010) – Bodyfelt et al., PRE (2011)]

Time evolution

H= **0.01, 0.2, 0.75**

W=4

Average over 1000 realizations!

$$\alpha(\log t) = \frac{d\langle \log m_2 \rangle}{d \log t}$$

Maximum Lyapunov Exponent (MLE)

Chaos: sensitive dependence on initial conditions.

Roughly speaking, the MLE of a given orbit characterizes the **mean exponential rate of divergence** of trajectories surrounding it.

Consider an orbit in the 2N-dimensional phase space with **initial condition x(0)** and **an initial deviation vector (small perturbation) from it v(0).**
Then the mean exponential rate of divergence is:

$$\text{MLE} = \lambda_1 = \lim_{t \to \infty} \Lambda(t) = \lim_{t \to \infty} \frac{1}{t} \ln \frac{\|v(t)\|}{\|v(0)\|}$$

$$\lambda_1 = 0 \rightarrow \text{Regular motion } (\Lambda \propto t^{-1})$$
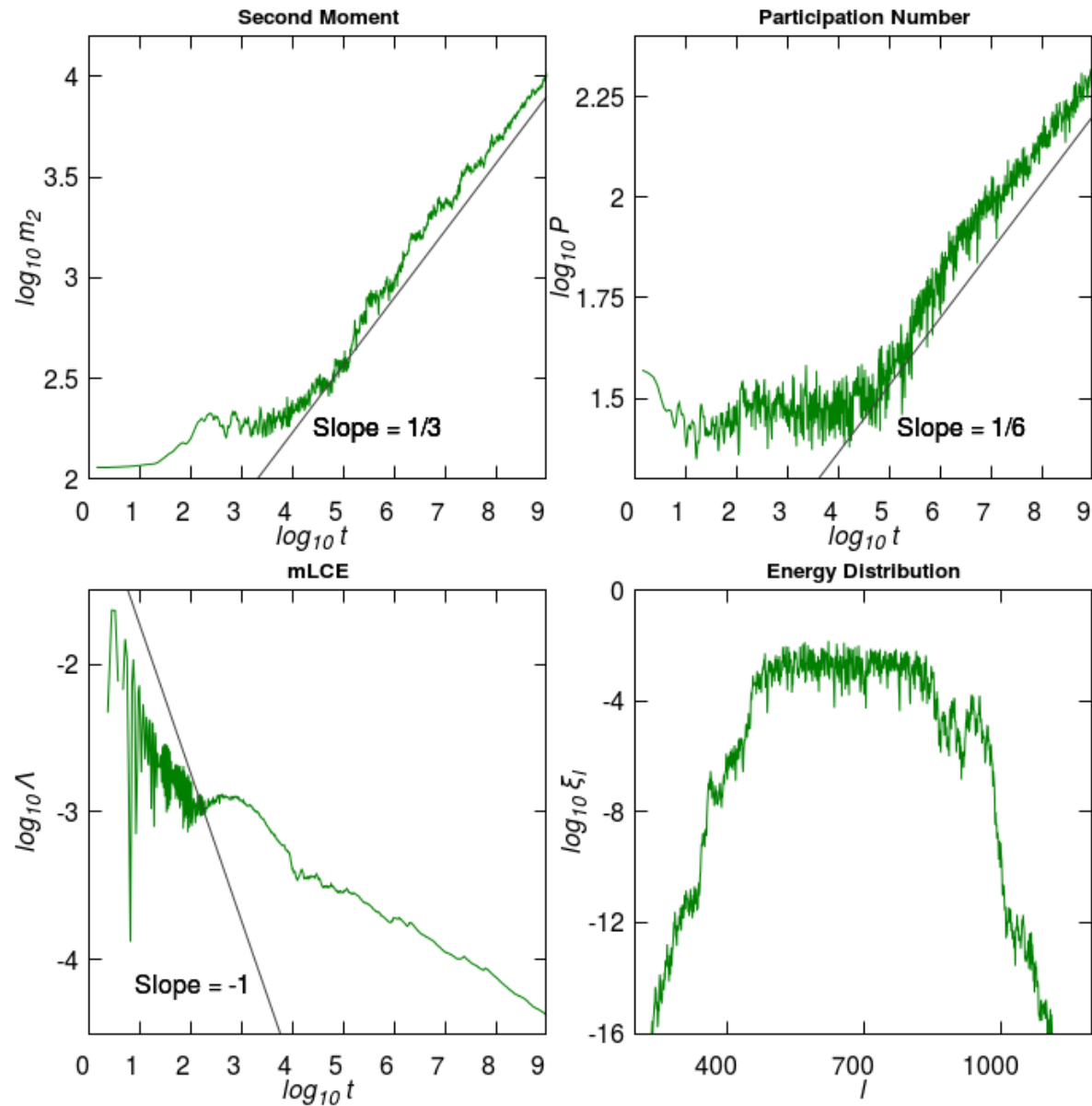$$\lambda_1 > 0 \rightarrow \text{Chaotic motion}$$

Figure 5.7. Behavior of σ_n at the intermediate energy $E = 0.125$ for initial points taken in the ordered (curves 1–3) or stochastic (curves 4–6) regions (after Benettin et al., 1976).
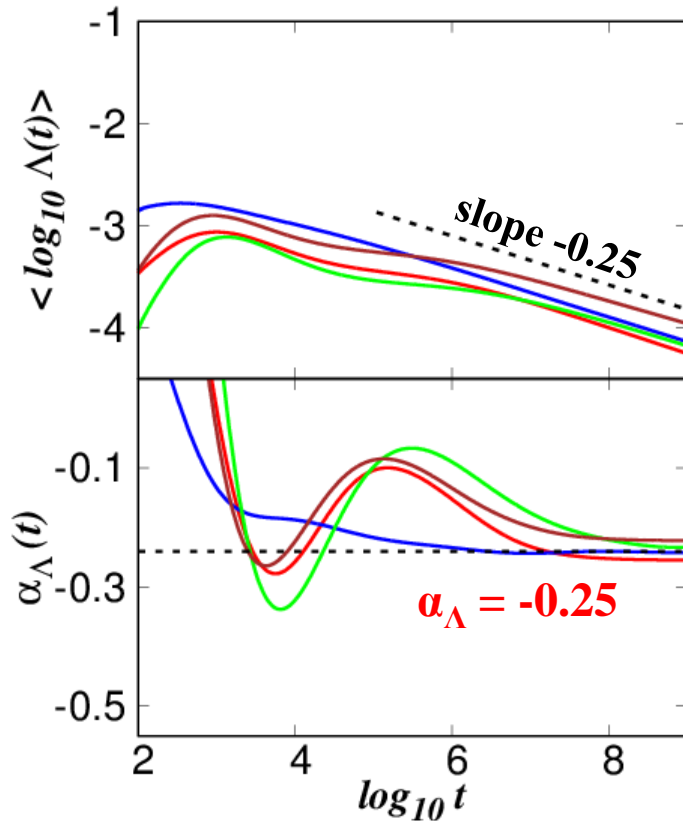
A weak chaos case

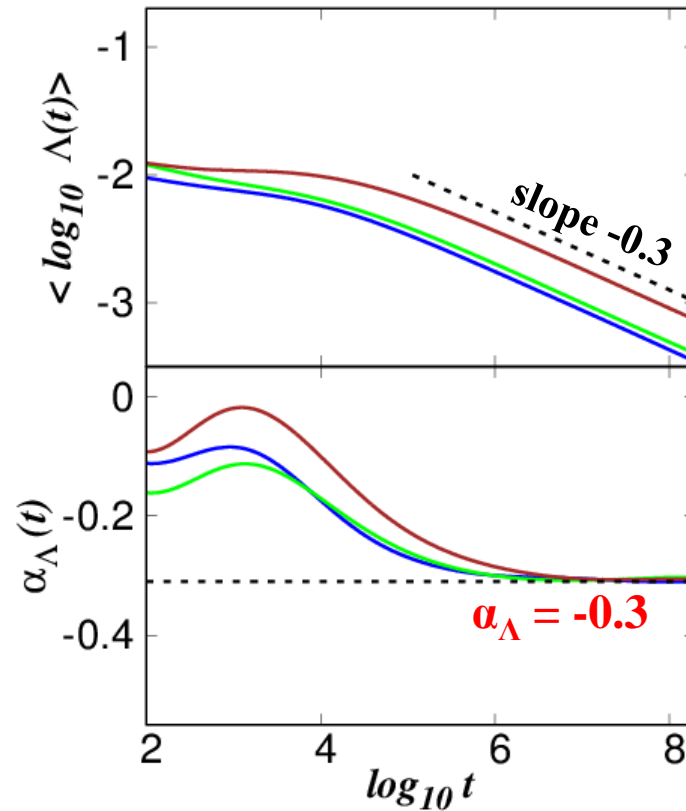**Block excitation L=37 sites, H=0.37, W=3.**

One disorder realization

Time evolution of the MLE: $\Lambda \propto t^{\alpha_\Lambda}$

Weak chaos (left panels)

Strong chaos (right panels)

slope -0.25

slope -0.3

$\alpha_\Lambda = -0.25$

$\alpha_\Lambda = -0.3$

Average over 100 realizations [Senyange et al., PRE (2018)]

Block excitation (L=37 sites) H=0.37, W=3

Single site excitation H=0.4, W=4

Block excitation (L=21 sites) H=0.21, W=4

Block excitation (L=13 sites) H=0.26, W=5

Block excitation (L=83 sites) H=0.83, W=2

Block excitation (L=37 sites) H=0.37, W=3

Block excitation (L=83 sites) H=0.83, W=3

The weak chaos case was also studied in S. et al., PRL (2013)

Deviation Vector Distributions (DVDs)

Energy DVD

Weak chaos L=37 sites, H=0.37, W=3

Deviation vector:
$v(t) = (\delta u_1(t), \delta u_2(t), \ldots, \delta u_N(t), \delta p_1(t), \delta p_2(t), \ldots, \delta p_N(t))$

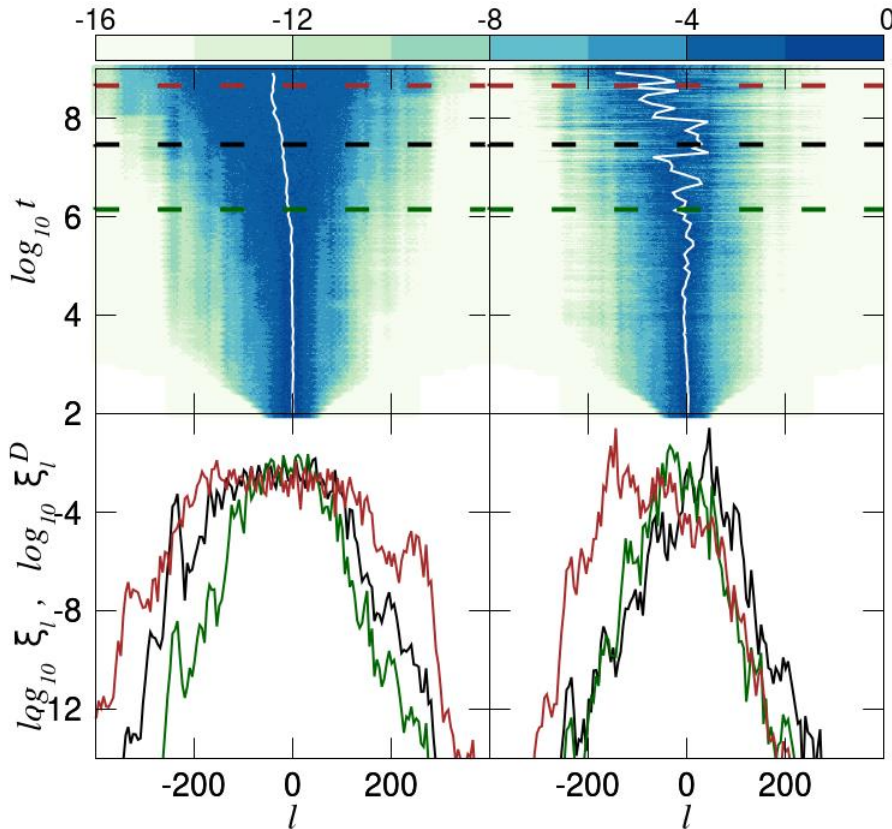**DVD:** $\xi_l^D = \dfrac{\delta u_l^2 + \delta p_l^2}{\sum_l \left(\delta u_l^2 + \delta p_l^2 \right)}$

DVDs: Weak and Strong Chaos

W=3, L=37, H=0.37
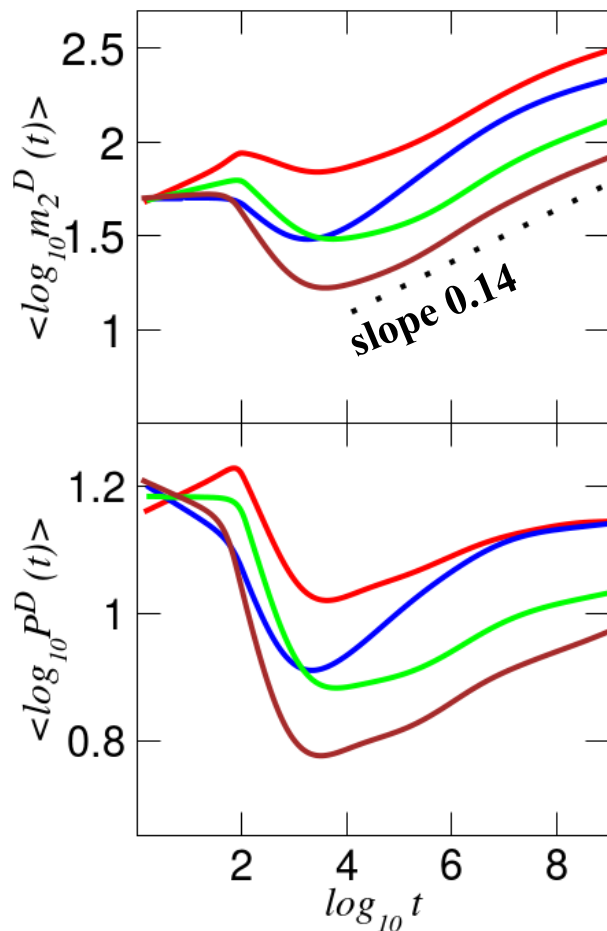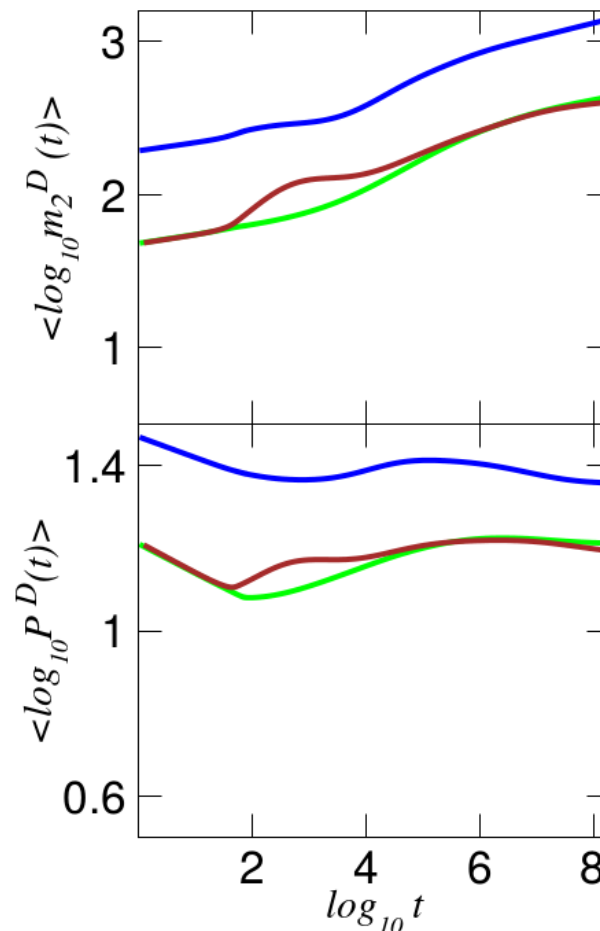
W=3, L=83, H=8.3

Chaotic hot spots meander through the system, supporting the homogeneity of chaos inside the wave packet.

Characteristics of DVDs
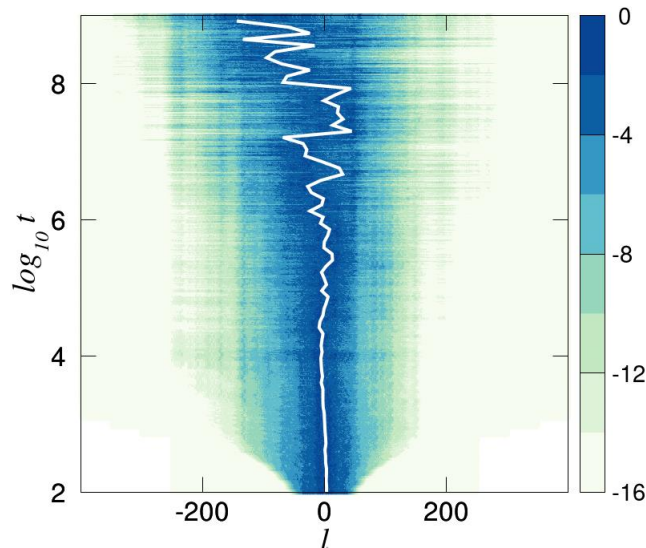
Weak chaos

Strong chaos

The DVD remains very concentrated: a rather small number of sites are highly chaotic at each time.

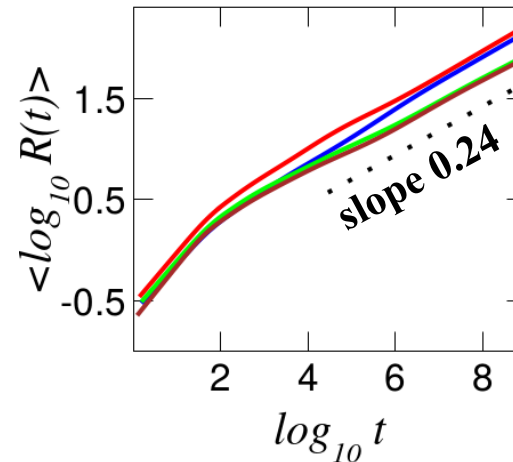# Characteristics of DVDs

**Weak chaos
L=37, H=0.37, W=3**
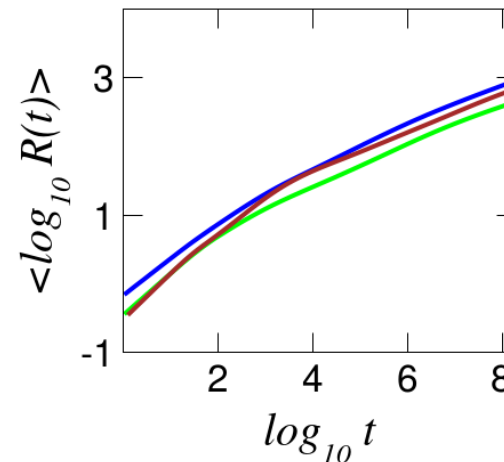

**Range of the lattice
visited by the DVD**

**Weak
chaos**

**Strong
chaos**

$$R(t) = \max_{[0,t]}\left\{\overline{l}_w(t)\right\} - \min_{[0,t]}\left\{\overline{l}_w(t)\right\}$$

$$\overline{l}_w = \sum_{l=1}^{N} l\,\xi_l^D$$

The DVD exhibits oscillations, whose amplitudes increase in time (larger amplitudes for strong chaos) in order to visit all regions inside the spreading wave packet.

Frequency Map Analysis (FMA)

Compute the **fundamental frequencies, f_1 and f_2,** of an observable related to the evolution of an orbit in **two successive time windows** of the same length, and check **whether or not these frequencies change in time** [Laskar, Icarus (1990) – Laskar et al., Physica D (1992) – Laskar, Physica D (1993) – Robutel & Laskar, Icarus (2000)].

Regular motion: The computed frequencies do not vary in time

Chaotic motion: The computed frequencies vary in time

For every lattice site l we compute the fundamental frequencies f_{1l} and f_{2l} for time windows of length $T = 6 \cdot 10^5$ time units and evaluate the **relative change of these two frequencies:**
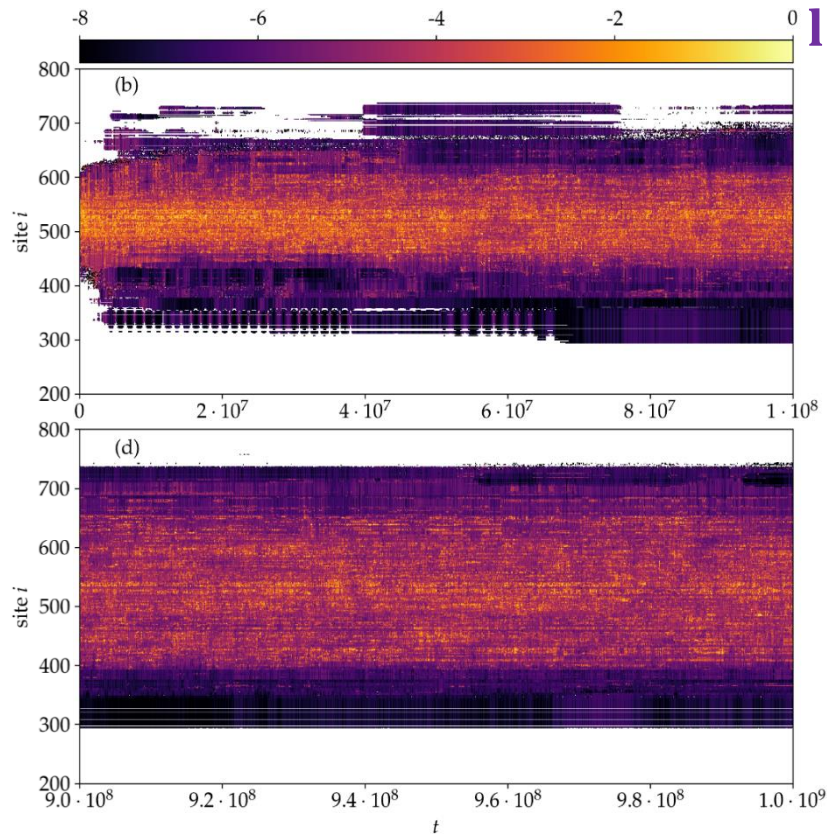
$$D_l = \left| \frac{f_{2l} - f_{1l}}{f_{1l}} \right|$$
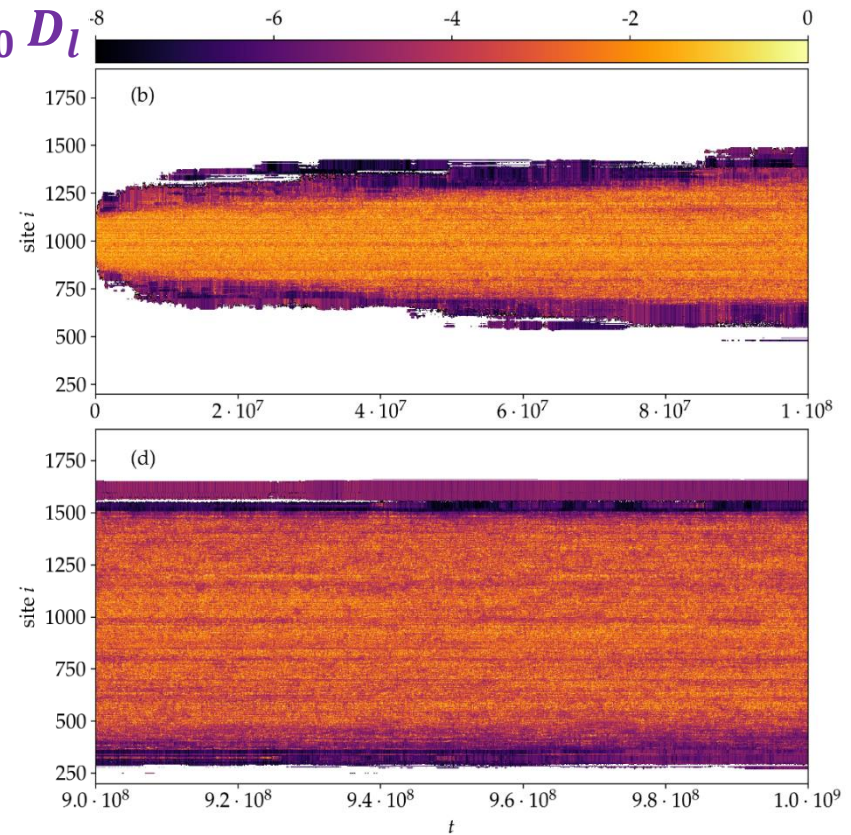
Regular motion: small D_l values

Chaotic motion: large D_l values

FMA: Weak and Strong Chaos

Weak chaos
L=1, H=0.4, W=4, N=999

Strong chaos
L=21, H=4.2, W=4, N=3499
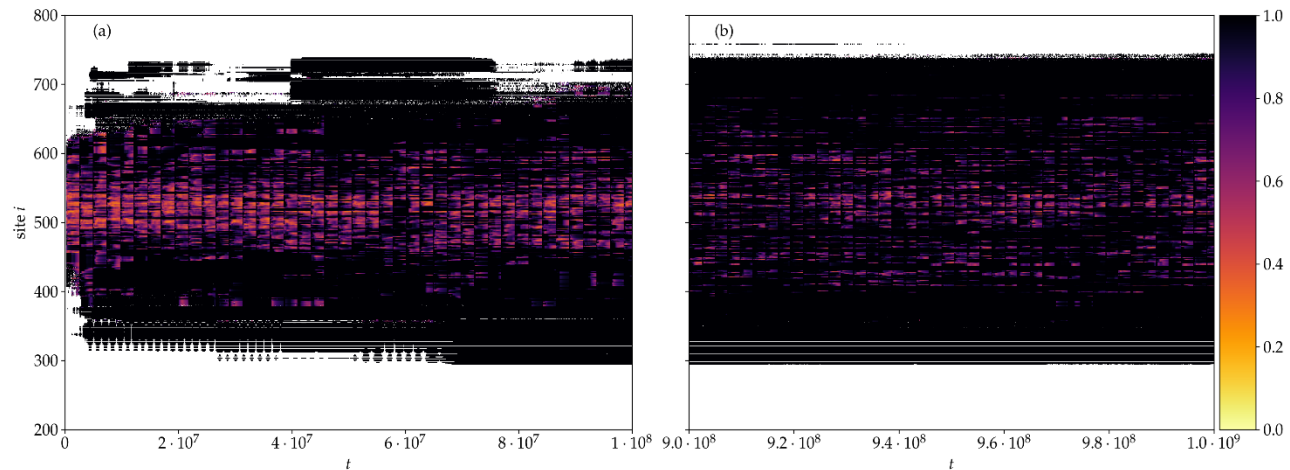
$\log_{10} D_l$

Chaotic behavior appears at the central regions of the wave packet, where the energy density is relatively large. The chaotic component of the wave packet **is more extended in the strong chaos case** [S. et al., IJBC (2022)]
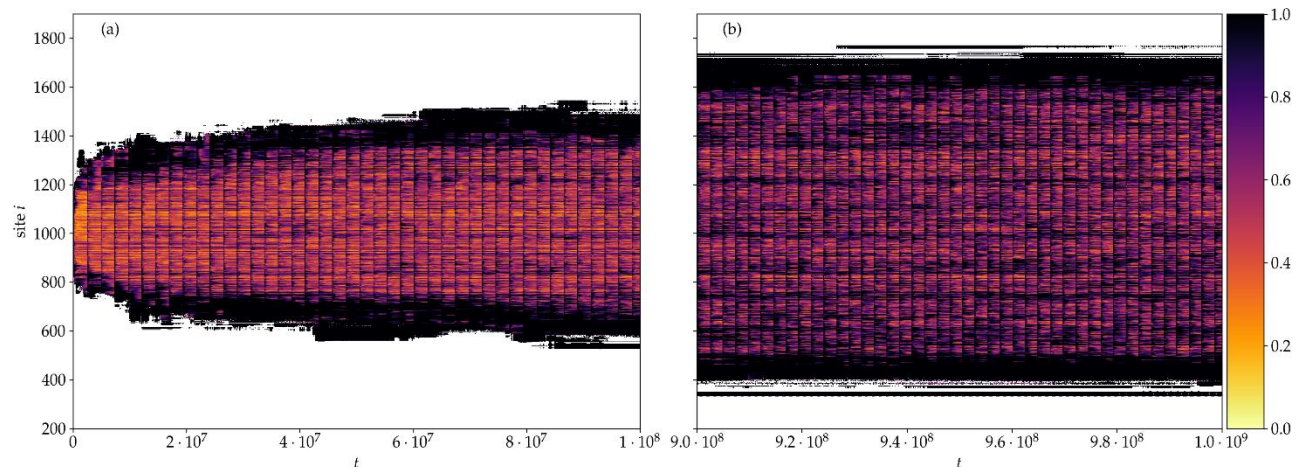
Frequency Locking (FL)

Frequency bins of width 10^{-4}. For each lattice site and a duration of $t = 2.4 \cdot 10^7$ we compute the fundamental frequencies in 200 time windows and register the related bins.

FL_l: the fraction of the most visited bin ($0 \le FL_l \le 1$). Measures the degree of practical frequency constancy (denoting nonchaotic behavior) of each oscillator.
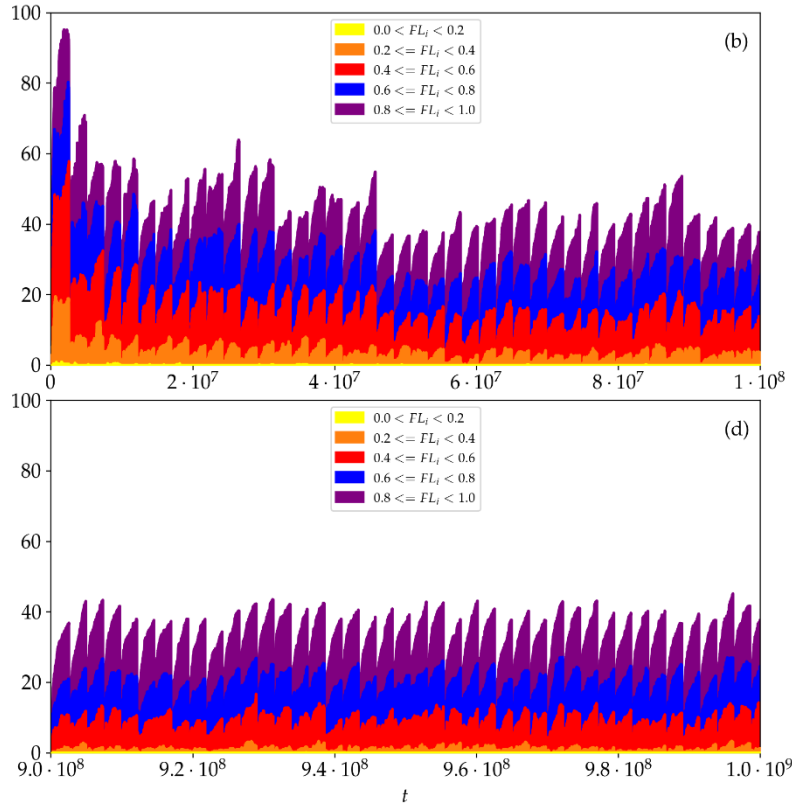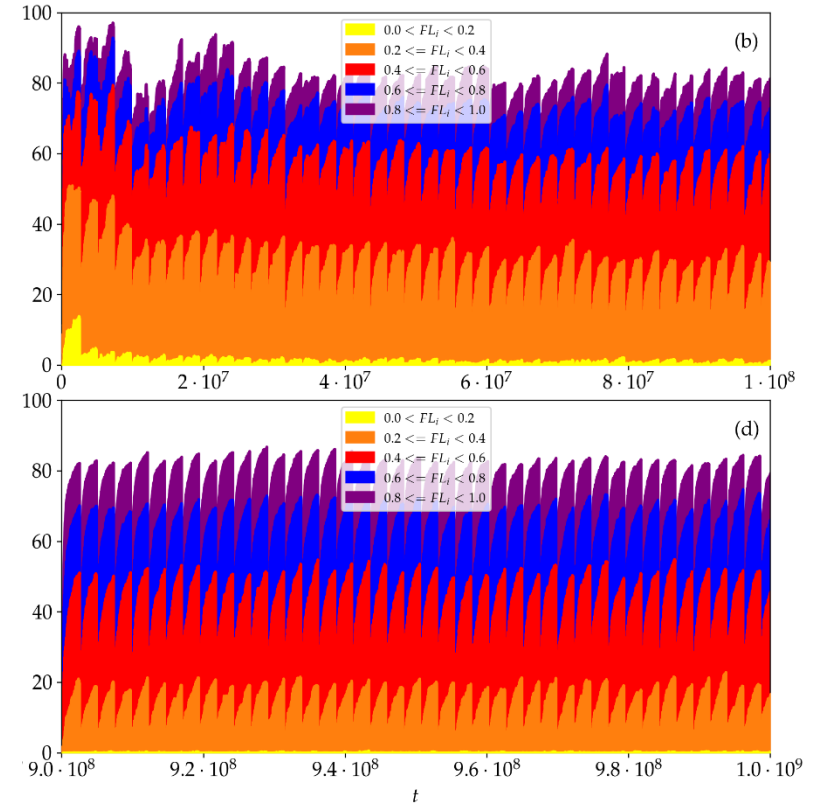
Weak chaos

Strong chaos

Frequency Locking (FL)

Accumulated percentages P_{FL} of sites with values in a particular FL range

Weak chaos

Strong chaos

The fraction of sites behaving chaotically is much larger in the strong chaos regime.

The percentage of strongly chaotic sites (having $FL_l < 0.4$) is about 5 times larger for strong chaos.

For both spreading regimes, the fraction of highly chaotic oscillators ($FL_l < 0.4$) decreases in time, although the percentage of chaotic sites remains practically constant.

The Generalized Alignment Index (GALI)

In the case of an N degree of freedom Hamiltonian system or a 2N symplectic map we follow the evolution of

k deviation vectors with 2≤k≤2N,

and define [S. et al., Physica D, (2007)] **the Generalized Alignment Index (GALI) of order k :**

$$GALI_k(t) = \|\widehat{v}_1(t) \wedge \widehat{v}_2(t) \wedge \dots \wedge \widehat{v}_k(t)\|$$

where

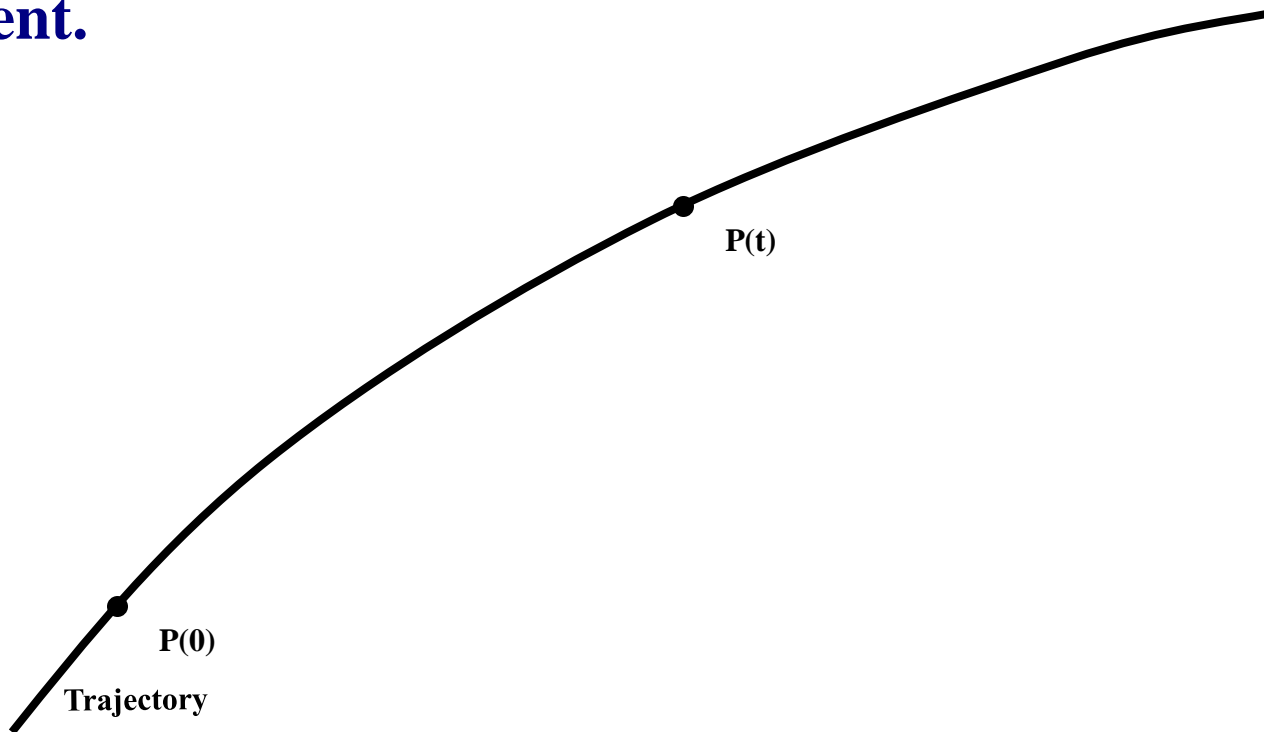$$\widehat{v}_1(t) = \frac{v_1(t)}{\|v_1(t)\|}.$$

GALI$_k$ is defined as **the volume of the parallelepiped** formed by the k normalized deviation vectors

Behavior of deviation vectors for chaotic motion

For chaotic orbits two initially different deviation vectors tend to coincide with the direction defined by the maximum Lyapunov exponent.
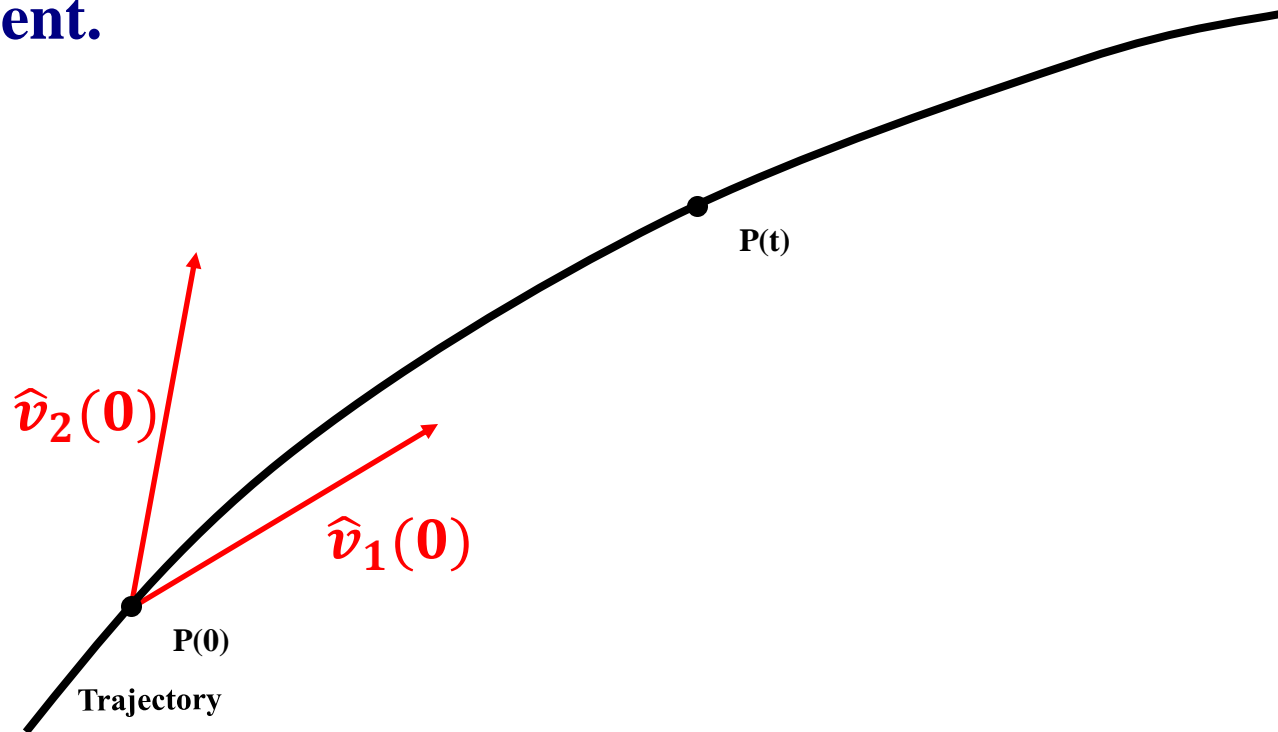
Behavior of deviation vectors for chaotic motion

For chaotic orbits two initially different deviation vectors tend to coincide with the direction defined by the maximum Lyapunov exponent.
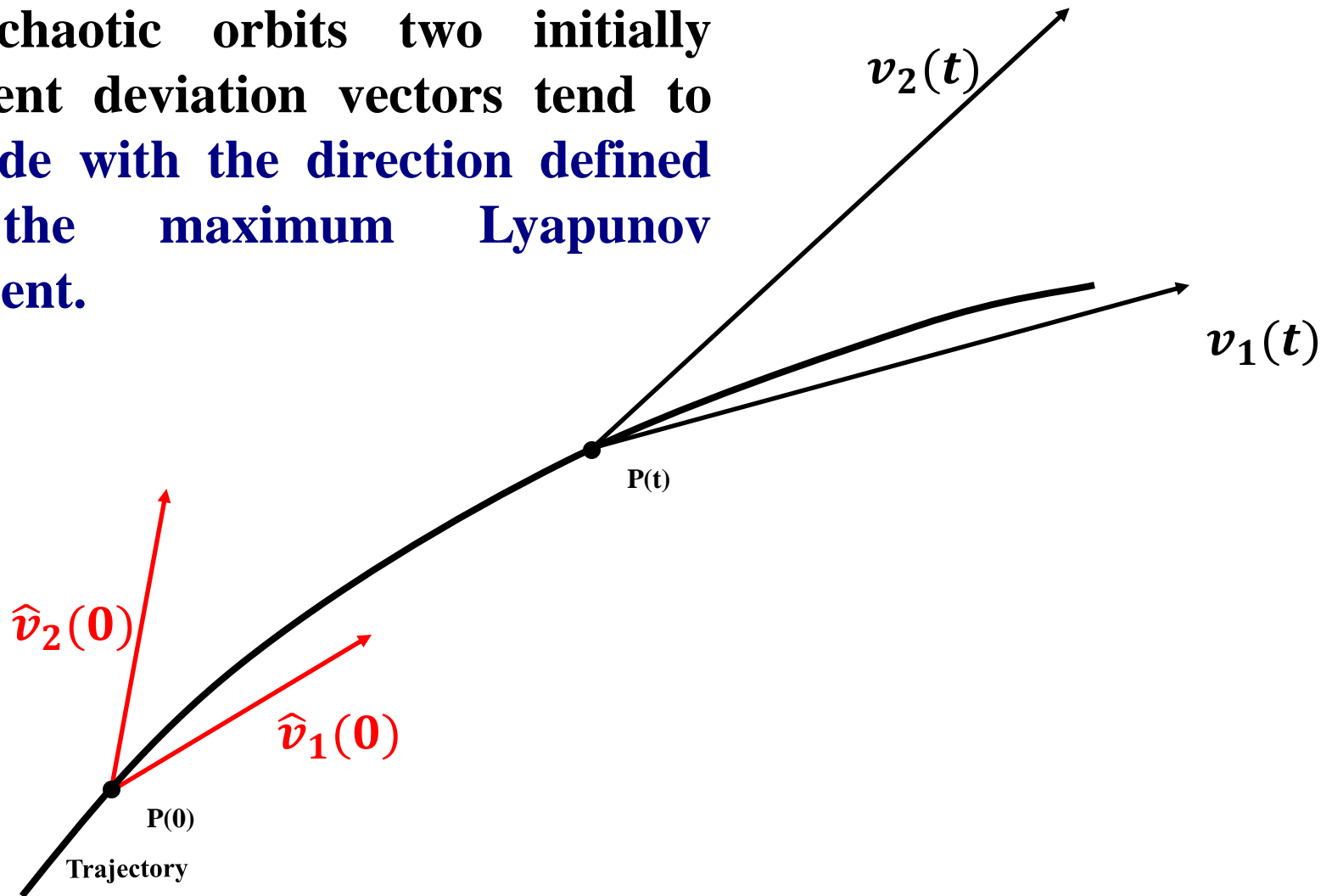
P(t)

P(0)

Trajectory

Behavior of deviation vectors for chaotic motion

For chaotic orbits two initially different deviation vectors tend to coincide with the direction defined by the maximum Lyapunov exponent.

$\widehat{v}_2(0)$

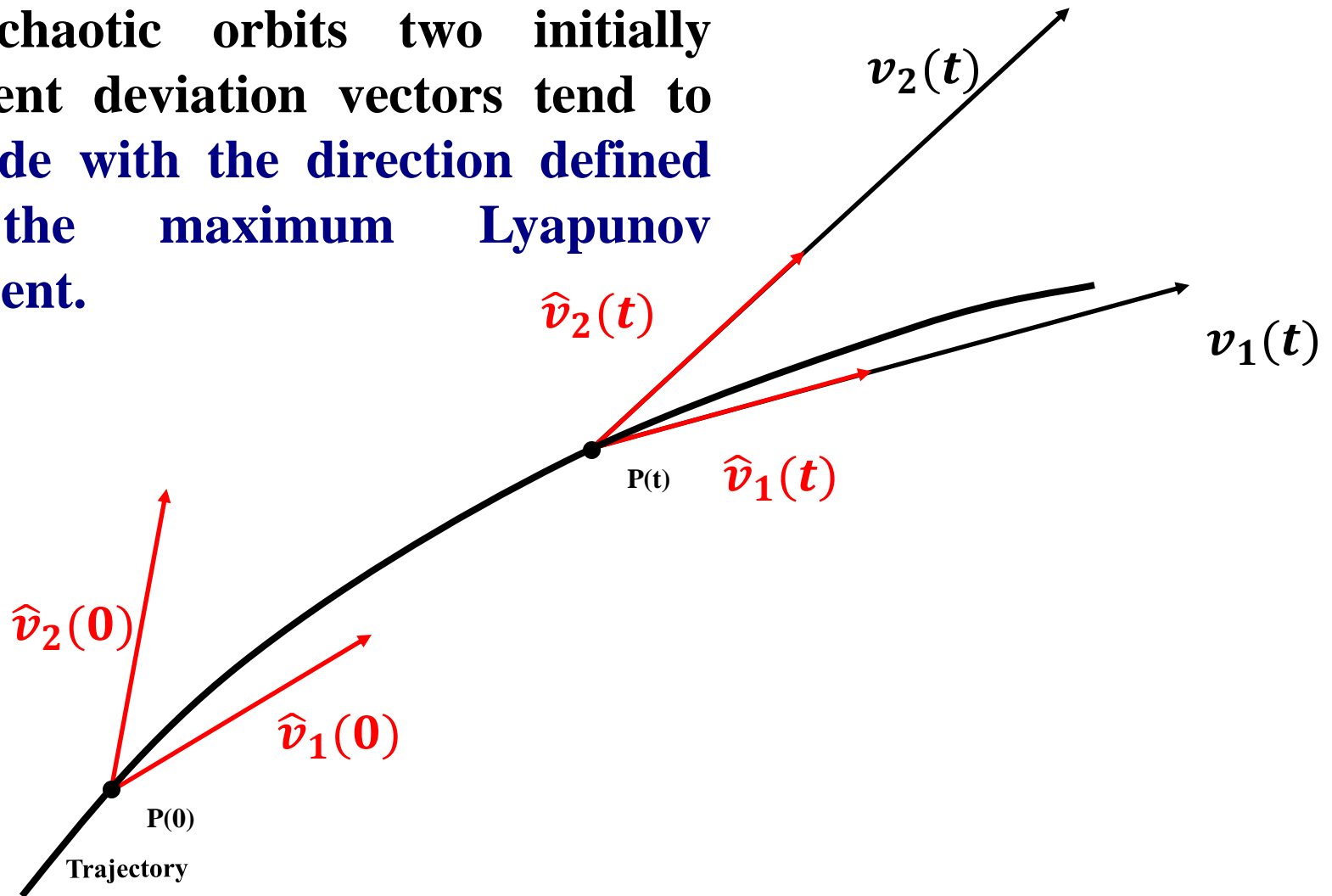$\widehat{v}_1(0)$

P(t)

P(0)

Trajectory

Behavior of deviation vectors for chaotic motion

For chaotic orbits two initially different deviation vectors tend to **coincide with the direction defined by the maximum Lyapunov exponent.**

$v_2(t)$

$v_1(t)$

P(t)

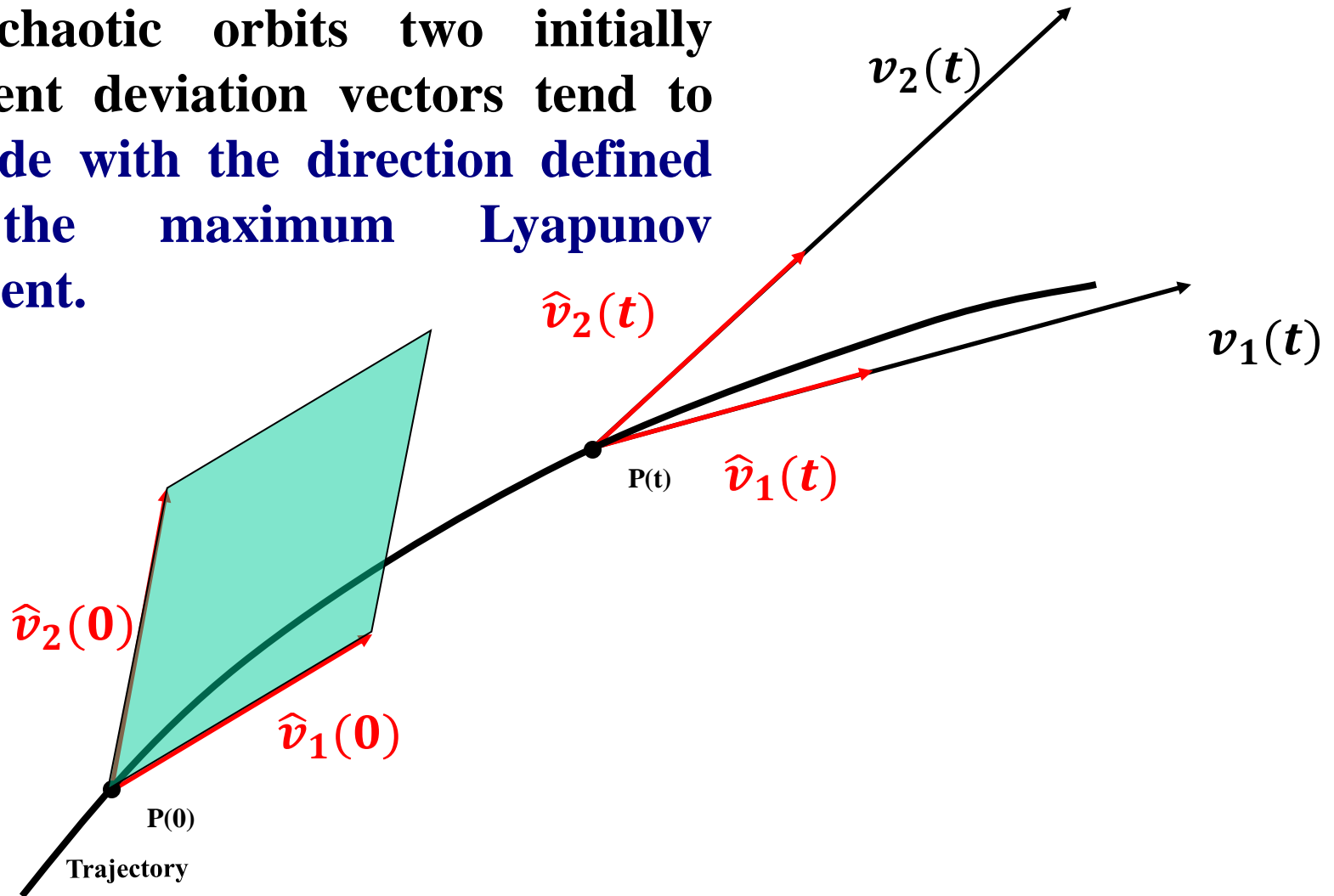$\widehat{v}_2(0)$

$\widehat{v}_1(0)$

P(0)

Trajectory

Behavior of deviation vectors for chaotic motion

For chaotic orbits two initially different deviation vectors tend to coincide with the direction defined by the maximum Lyapunov exponent.
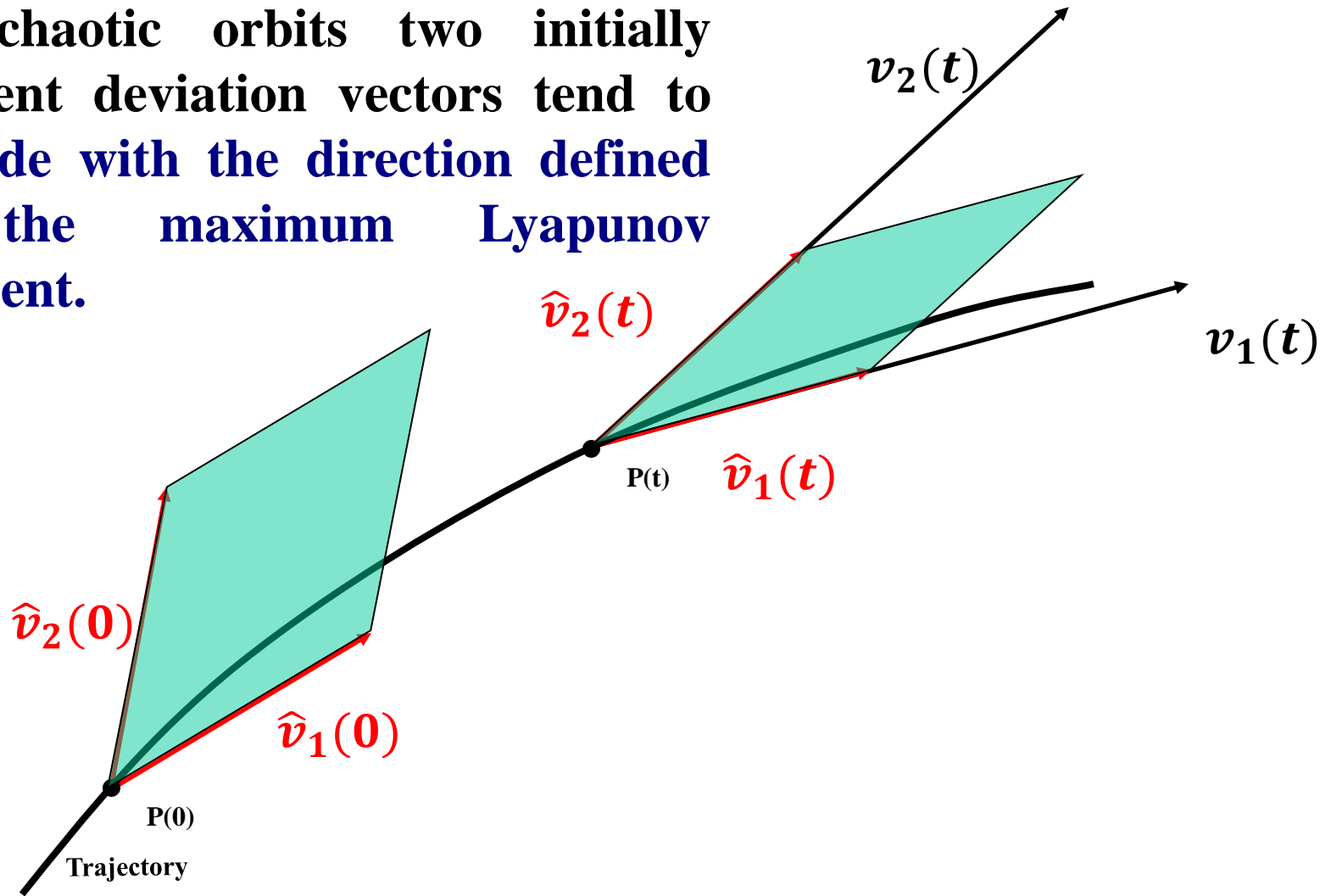
Behavior of deviation vectors for chaotic motion

For chaotic orbits two initially different deviation vectors tend to coincide with the direction defined by the maximum Lyapunov exponent.

Behavior of deviation vectors for chaotic motion

For chaotic orbits two initially different deviation vectors tend to **coincide with the direction defined by the maximum Lyapunov exponent.**

$v_2(t)$

$\widehat{v}_2(t)$

$v_1(t)$

P(t)

$\widehat{v}_1(t)$

$\widehat{v}_2(0)$

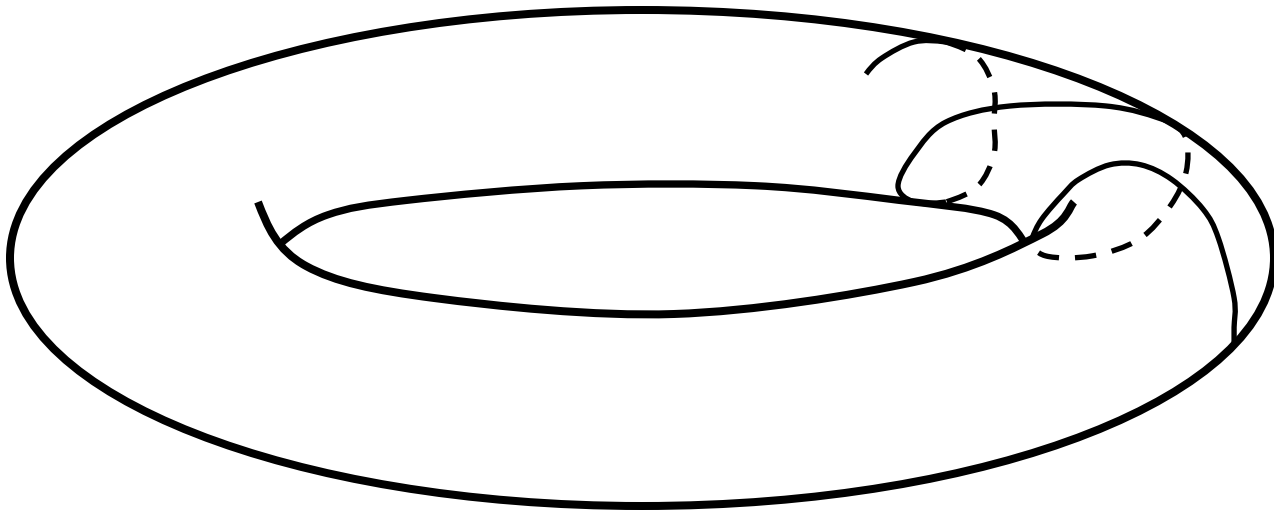$\widehat{v}_1(0)$

P(0)

Trajectory

Behavior of deviation vectors for regular motion

Regular motion occurs on a torus and two different initial deviation vectors **become tangent to the torus, generally having different directions.**

Behavior of deviation vectors for regular motion

Regular motion occurs on a torus and two different initial deviation vectors **become tangent to the torus, generally having different directions.**
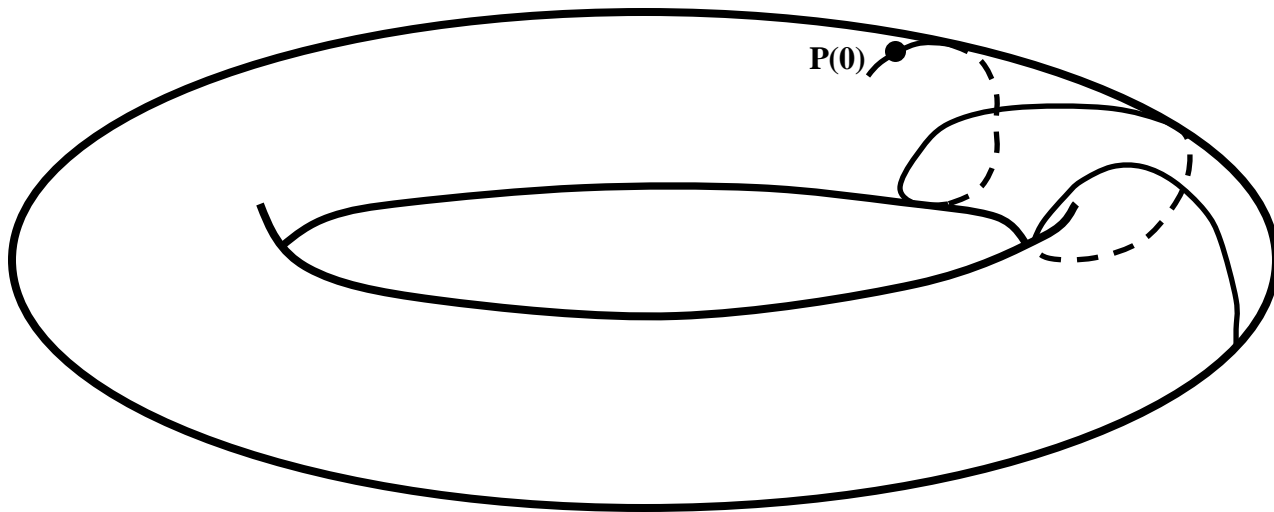
Behavior of deviation vectors for regular motion

Regular motion occurs on a torus and two different initial deviation vectors **become tangent to the torus, generally having different directions.**
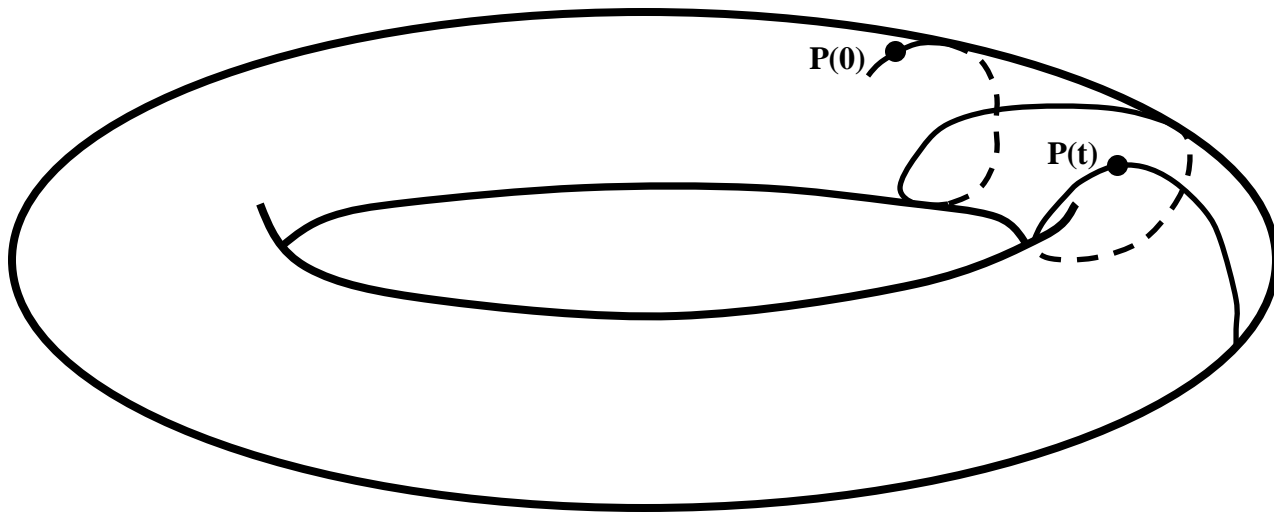
Behavior of deviation vectors for regular motion

Regular motion occurs on a torus and two different initial deviation vectors become tangent to the torus, generally having different directions.

Behavior of deviation vectors for regular motion

Regular motion occurs on a torus and two different initial deviation vectors become tangent to the torus, generally having different directions.
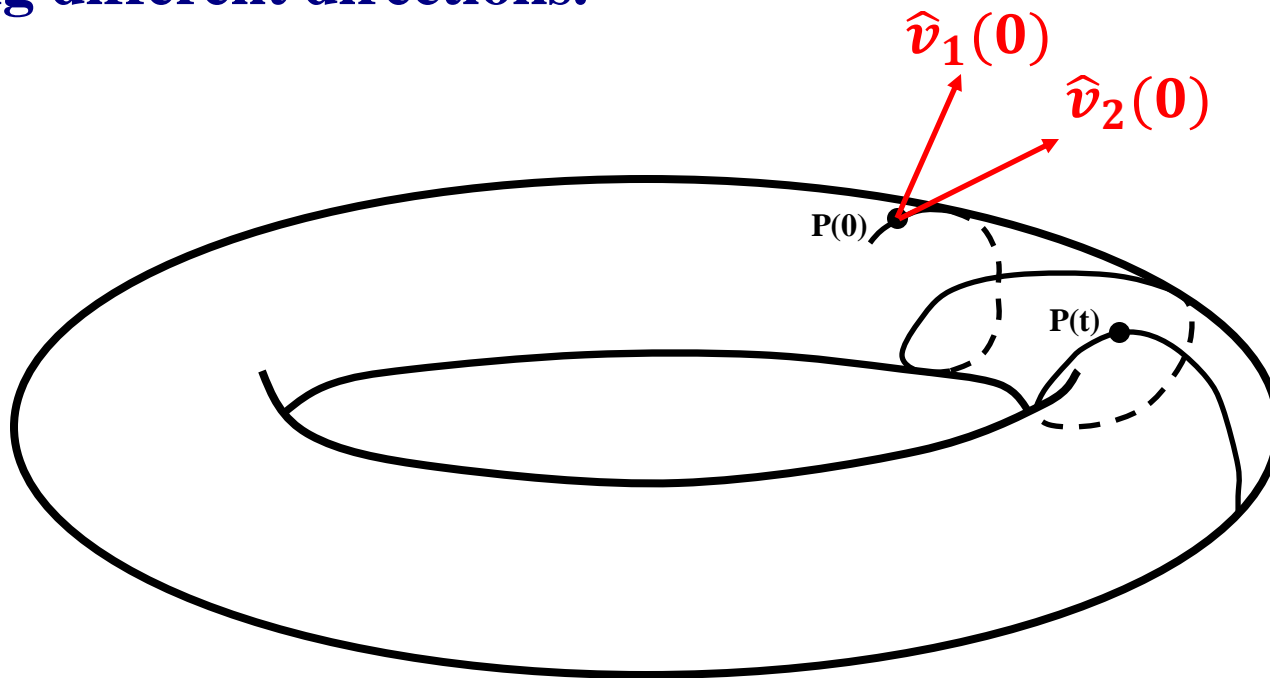
Behavior of deviation vectors for regular motion

Regular motion occurs on a torus and two different initial deviation vectors become tangent to the torus, generally having different directions.
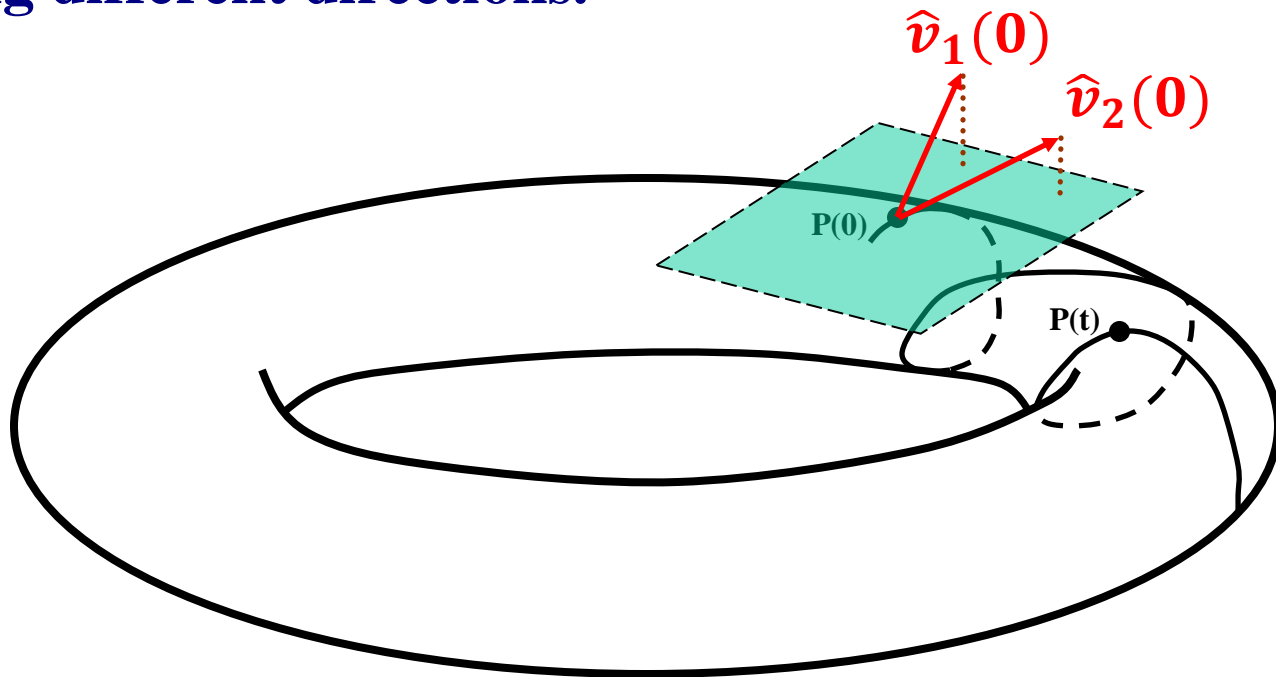
Behavior of deviation vectors for regular motion

Regular motion occurs on a torus and two different initial deviation vectors become tangent to the torus, generally having different directions.
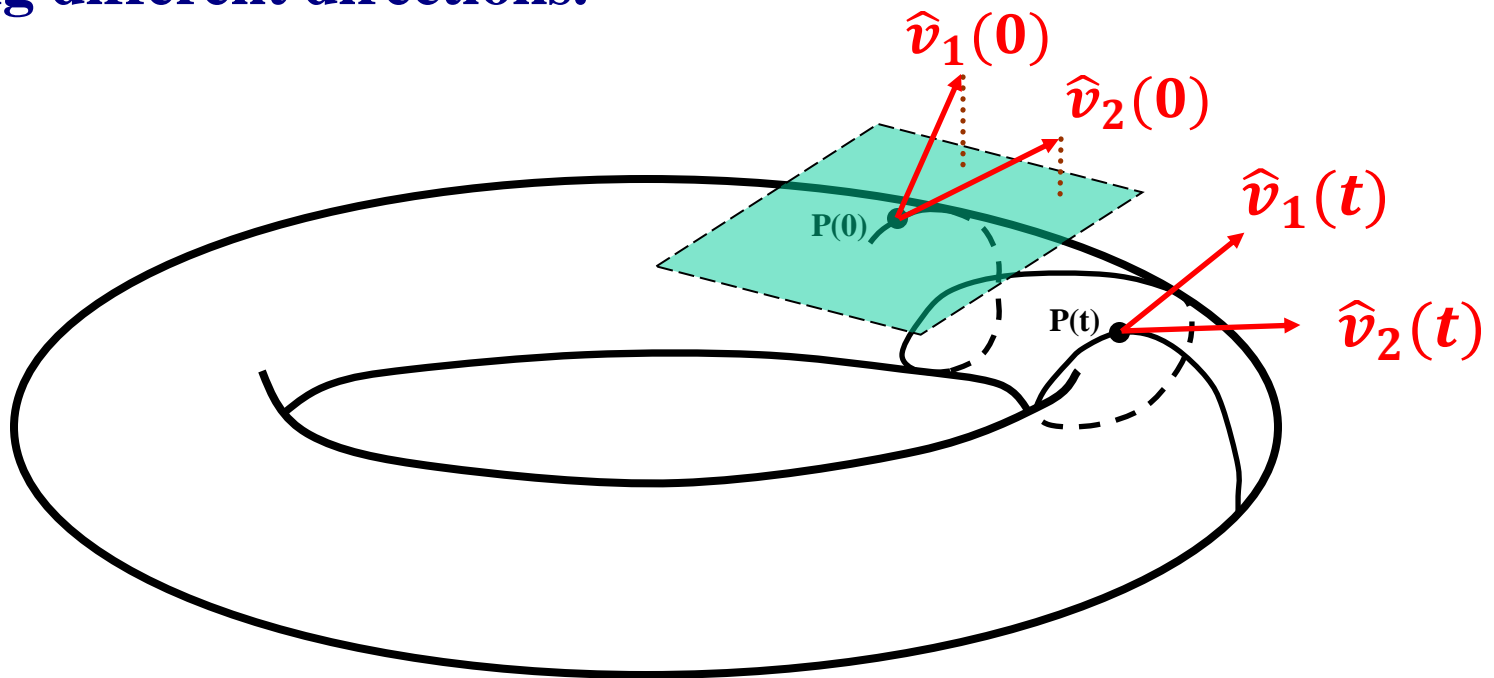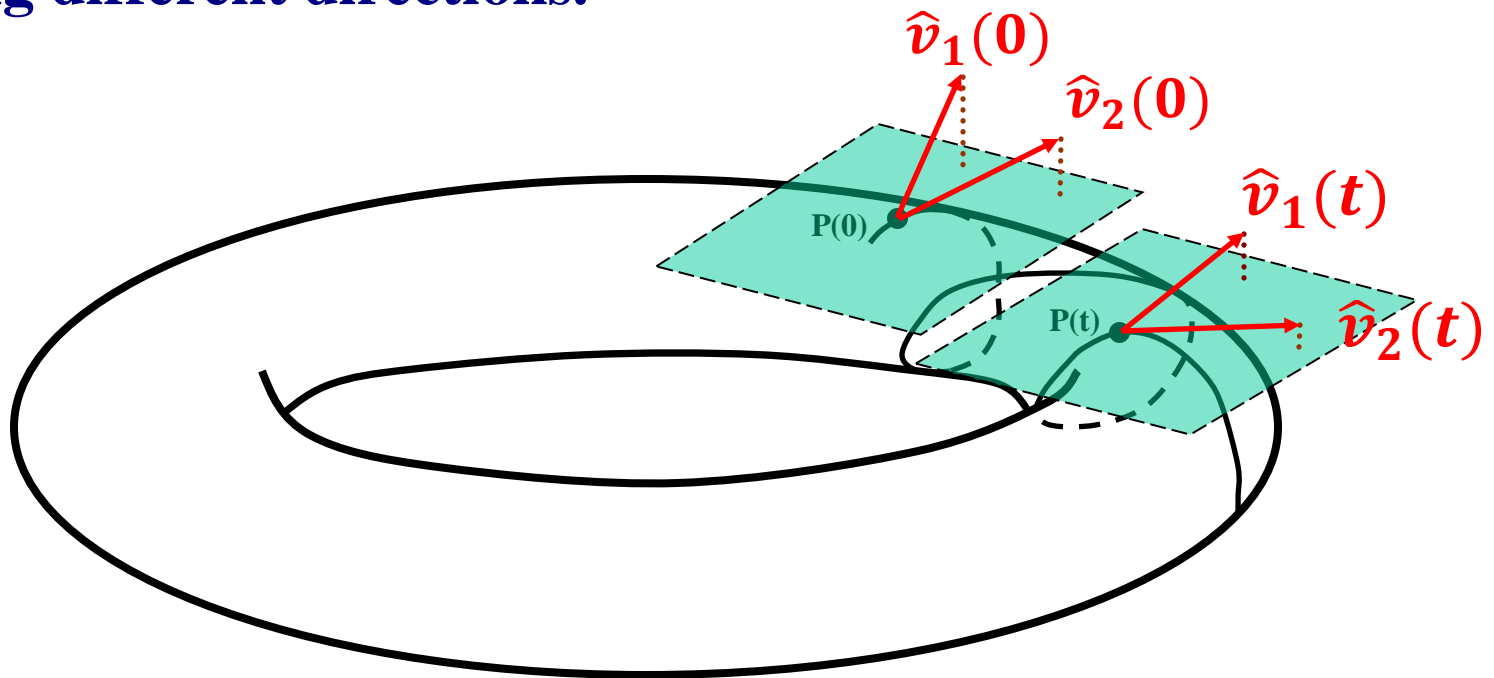
Behavior of deviation vectors for regular motion

Regular motion occurs on a torus and two different initial deviation vectors become tangent to the torus, generally having different directions.

Behavior of the GALI$_k$

Chaotic motion: GALI$_k$ ($2 \leq k \leq 2N$) tends exponentially to zero with exponents which involve the values of the first k largest Lyapunov exponents $\lambda_1, \lambda_2, \ldots, \lambda_k$:

$$GALI_k(t) \propto e^{-[(\lambda_1-\lambda_2)+(\lambda_1-\lambda_3)+\ldots+(\lambda_1-\lambda_k)]t}$$
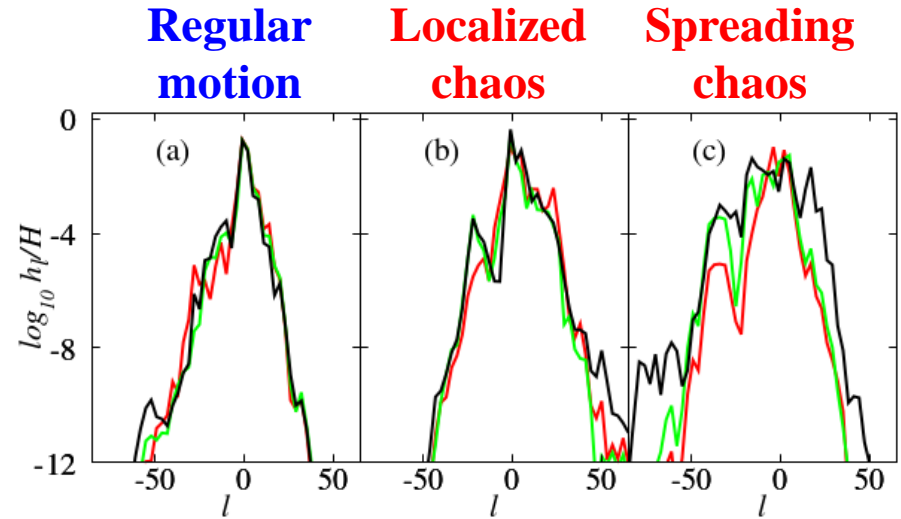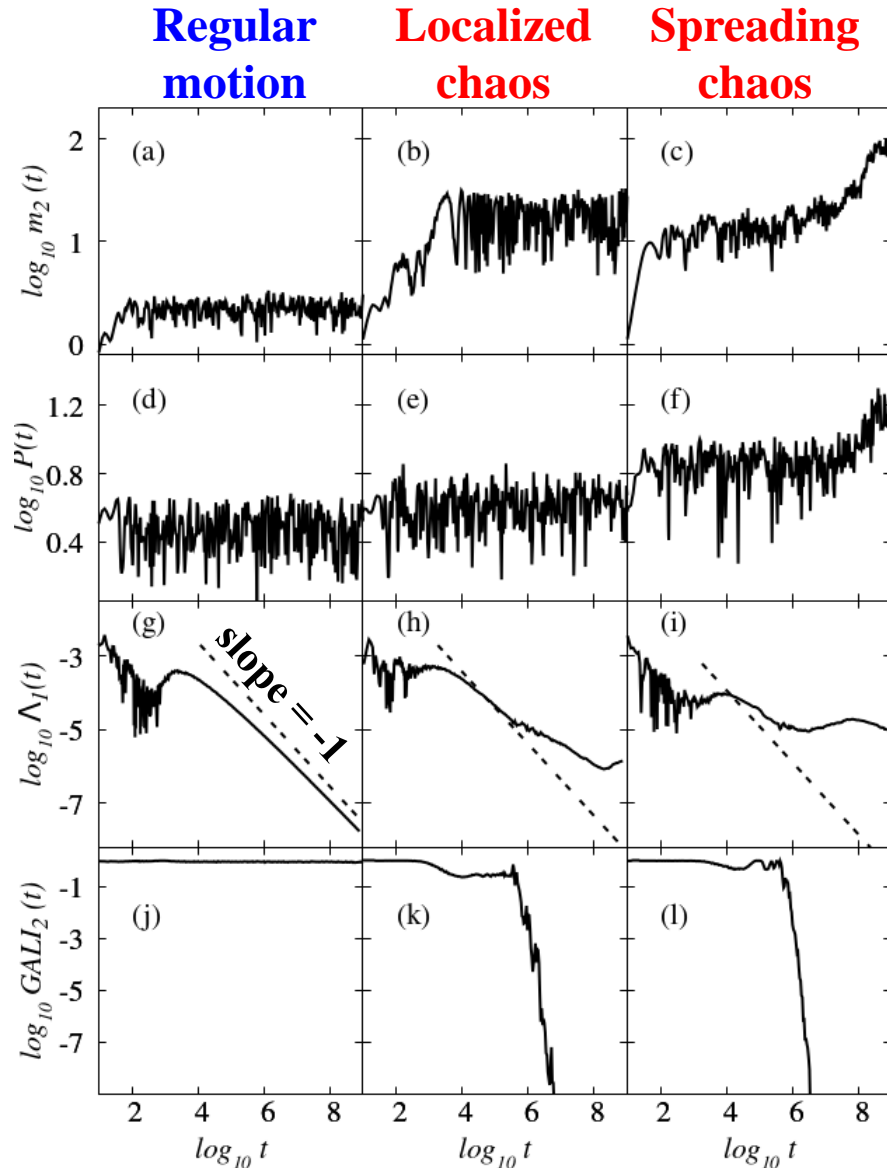
Regular motion: When the motion occurs on an **N-dimensional torus** then the behavior of GALI$_k$ is given by [S. et al., Eur. Phys. J. Sp. Top. (2008)]:

$$GALI_k(t) \propto \begin{cases} \text{constant} & \text{if} \quad 2 \leq k \leq N \\ \dfrac{1}{t^{2(k-N)}} & \text{if} \quad N < k \leq 2N \end{cases}$$

Here we only consider **GALI$_2$ (k=2)** which is equivalent to the **Smaller Alignment Index (SALI)** [S, J. Phys A (2001)].

Regular vs. chaotic (localized or spreading) motion

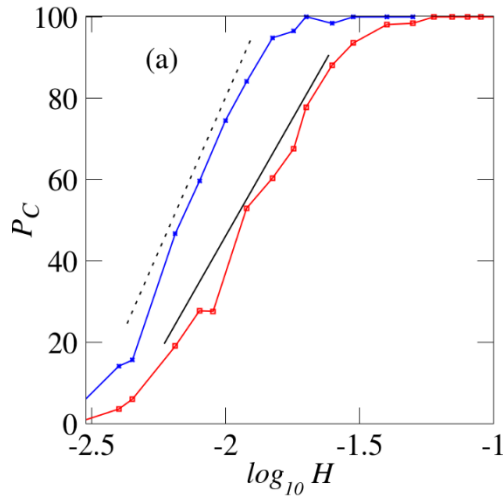**Different disorder realizations can exhibit different behaviors.**

$t = \mathbf{10^5}, \mathbf{10^7}, \mathbf{10^9}$

Single site excitations, L=1, for W=6, H=0.02 [Senyange & S., Physica D (2022)].

The GALI$_2$ can identify chaos much more clearly than the MLE.

Decreasing nonlinearity

Single site excitations

Single mode excitations

P_C: % of chaotic orbits

W=4, W=6

P_{CL}: % of localized chaos P_{CS}: % of spreading chaos

Energy thresholds for transition to regular motion and to spreading chaos are lower for single site excitations which permit mode interactions [Senyange & S., Physica D (2022)].

Summary

We investigated in depth the spatiotemporal chaotic behavior of the DKG multidimensional Hamiltonian system.

- **Identification of 2 different dynamical spreading regimes: weak and strong chaos**

- **The MLE reveals the decrease of the system's chaoticity in time**

  Weak chaos: $\Lambda \propto t^{-0.25}$ - Strong chaos: $\Lambda \propto t^{-0.30}$

- **The DVDs provide information about the propagation of chaos**

  Wandering of localized chaotic hot spots in the lattice's excited part homogenize chaos.

- **FMA computations uncover the characteristics of chaos evolution**

  Chaotic behavior appears at the central regions of the wave packet, being more pronounced in the strong chaos case.

- **The GALI method allows the detailed study of the system's behavior when it approaches its linear limit**

  Clear identification of chaos.

  Efficient distinction between localized and spreading chaos.

  Identification of energy thresholds leading to global chaotic spreading and to the total absence of chaos.

Main references

- **S. (2001) J. Phys. A, 34, 10029**
- **S., Bountis, Antonopoulos (2007) Physica D, 231, 30**
- **S., Bountis, Antonopoulos (2008) Eur. Phys. J. Sp. Top., 165, 5**
- **Flach, Krimer, S. (2009) PRL, 102, 024101**
- **S., Flach (2010) PRE, 82, 016208**
- **Laptyeva, Bodyfelt, Krimer, S., Flach (2010) EPL, 91, 30001**
- **Bodyfelt, Laptyeva, S., Krimer, Flach (2011) PRE, 84, 016205**
- **S., Gkolias, Flach (2013) PRL, 111, 064101**
- **Senyange, Many Manda, S. (2018) PRE, 98, 052229**
- **Senyange, S. (2022) Physica D, 432, 133154**
- **S., Gerlach, Flach (2022) Int. J. Bifurc. Chaos, 32, 2250074**